Isparta Uygulamalı Bilimler Üniversitesi
Ziraat Fakültesi Dergisi
ISSN 1304-9984

Research Article/Araştırma Makalesi

Ziraat Fakültesi Dergisi,
Cilt 17, Sayı 2,
Sayfa 95-103, 2022

Journal of the Faculty of Agriculture
Volume 17, Issue 2,
Page 95-103, 2022

Determination of Olive Tree (*Olea europaea L.*) Some Dendrometric Components from Unmanned Aerial Vehicle (UAV) Data with Local Extrema and Multiresolution Segmentation Algorithms

Mesut ÇOŞLU[1], Namık Kemal SÖNMEZ*[2]

Abstract: In this study, it was aimed to determine the dendrometric components of olive trees by using an unmanned aerial vehicle (UAV). The research was carried out in the olive groves of Akdeniz University Faculty of Agriculture. The study consists of the basic stages of acquisition, processing and analysis of UAV images. In the first stage, autonomous flight was performed with the UAV and digital images of the area were collected. In addition, at this stage, the number and height of olive trees in the area were determined by making local measurements. In the second stage, orthomosaic image, digital surface model (DSM) and digital terrain model (DTM) were produced by processing UAV images. At this stage, tree crown boundaries were determined by manual digitization over the orthomosaic image. Then, a canopy height model (CHM) was created to semi-automatically calculate the crown borders, number of trees and tree height values of olive trees. As a result of the evaluation of semi-automatic findings and ground measurements, the general accuracy in the determination of trees in the olive grove was 96.15%, the accuracy of the producer was 85.14% and the user accuracy was 81.82% in the determination of the tree crown boundaries. In addition, high correlations were obtained in the determination of tree crown area (r = 0.980) and tree height (r = 0.918). According to these results, it has been revealed that some dendrometric components of the olive tree can be determined quite successfully with the semi-automatically calculated data from the UAVs.

Keywords: Canopy height model, olive tree, precision farming, UAV

İnsansız Hava Aracı (İHA) Verilerinden Zeytin Ağacının (Olea europaea L.) Bazı Dendrometrik Bileşenlerinin Yerel Ekstrema ve Çoklu Çözünürlüklü Bölütleme Algoritmaları ile Belirlenmesi

Öz: Bu çalışmada, insansız hava aracı (İHA) kullanılarak zeytin ağaçlarının dendrometrik bileşenlerin belirlenmesi amaçlanmıştır. Araştırma Akdeniz Üniversitesi Ziraat Fakültesi zeytinliklerinde gerçekleştirilmiştir. Çalışma, İHA görüntülerinin elde edilmesi, işlenmesi ve analizi temel aşamalarından oluşmaktadır. İlk aşamada İHA ile otonom uçuş gerçekleştirilerek alanın dijital görüntüleri toplanmıştır. Ayrıca bu aşamada yersel ölçümler yapılarak alandaki zeytin ağaçlarının sayısı ve yükseklikleri belirlenmiştir. İkinci aşamada, İHA görüntüleri işlenerek ortomozaik görüntü, sayısal yüzey modeli (DSM) ve sayısal arazi modeli (DTM) üretilmiştir. Bu aşamada ortomozaik görüntü üzerinden manuel sayısallaştırma ile ağaç taç sınırları belirlenmiştir. Daha sonra zeytin ağaçlarının taç sınırlarını, ağaç sayısını ve ağaç yükseklik değerlerini yarı otomatik olarak hesaplamak için bir kanopi yükseklik modeli (KYM) oluşturulmuştur. Yarı otomatik bulgular ile yersel ölçümlerin değerlendirilmesi sonucunda zeytinlikteki ağaçların tespitinde genel doğruluk %96,15, ağaç taç sınırlarının belirlenmesinde ise üretici doğruluğu %85.14 ve kullanıcı doğruluğu %81.82 olarak bulunmuştur. Ayrıca ağaç taç alanı (r = 0.980) ve ağaç yüksekliğinin (r = 0.918) belirlenmesinde de yüksek korelasyonlar elde edilmiştir. Bu sonuçlara göre, İHA'lardan yarı otomatik olarak hesaplanan veriler ile zeytin ağacının bazı dendrometric bileşenlerinin oldukça başarılı bir şekilde belirlenebildiği ortaya konmuştur.

Anahtar Kelimeler: Kanopi yükseklik modeli, zeytin ağacı, hassas tarım, İHA

Sorumlu yazar (Corresponding author)
nksonmez@akdeniz.edu.tr

Alınış (Received): 28/07/2022
Kabul (Accepted): 16/09/2022

[1]Akdeniz University, Institute of Natural and Applied Sciences, Department of Remote Sensing and Geographic Information Systems, Antalya, Türkiye

[2]Akdeniz University, Faculty of Science, Department of Space Science and Technologies Faculty of Science, Antalya, Türkiye

DOI: 10.54975/isubuzfd.1150068

1. Introduction

The increasing world population in recent years has also affected the increase in food demand. Increasing food demand and, more importantly, difficulties in accessing quality food have brought some problems to the agenda. The most important of these problems is the ones experienced in sustainable agricultural practices. Precision agriculture is the most effective use of resources in order to ensure sustainability in agricultural production. While resources are used effectively in precision agriculture, it is aimed to minimize environmental effects and increase yield and quality at the same time. Today, studies on precision agriculture applications continue to increase (Carolan, 2017; Das, 2018; Dong et al., 2020).

Remote sensing, which is also defined as the technology of obtaining remote information about an object under investigation, is also frequently used in studies carried out within the scope of agricultural applications (Sunar et al., 2013). Remote sensing platforms are considered as a tool for precision agriculture. The increase in spatial, spectral and temporal resolutions of remote sensed data has also increased the use of this technology in agricultural production areas. Although satellite data, which is frequently used in remote sensing studies, is successfully used in the mapping and monitoring of agricultural production areas, the temporal and spatial resolutions of satellite data for agricultural applications are not sufficient in some cases. For this reason, UAVs have been used frequently in agricultural research in recent years, especially with their low cost and high flexibility capabilities. The most important disadvantage of UAVs, which are very advantageous compared to satellites, is that they have smaller coverage areas. It can be more advantageous to work with UAVs, especially in areas smaller than 5 hectares where precision farming practices are applied (Matese et al., 2013).

Unmanned aerial vehicles are frequently used in precision agriculture because they provide data with higher spatial resolution. Studies using unmanned aerial vehicles include determination of plant heights of wheat of different genotypes under field conditions with low altitude imaging performed by Demir et al., (2018), semi-automatic calculation of plant heights of durum wheat variety shot on three different dates with UAVs with different characteristics by Sönmez et al., (2021), and approaches to automatically finding citrus trees from the digital surface model produced from the images taken from the UAV can be given as examples (Ok and Özdaracı-Ok, 2017).

Unmanned aerial vehicles can also be used in the management of orchards. Orchard management is essentially monitoring the garden and following the trees in the garden. The operations carried out in this context are the measurement of tree parameters and the monitoring of the change and development in these parameters. This is only possible by tracking and following the trees in the garden on an individual tree basis. For this reason, UAVs that can provide instant data with higher spatial and temporal resolution for trees in orchards can be used for this purpose.

For the determination of trees in the orchard, Ok and Ozdarici-Ok (2018) presented an approach for the detection of citrus trees using photogrammetric DSMs based on UAV images. The researchers found that their method had an overall accuracy of 91.1% in a pixel-based analysis and 97.5% in an object-based analysis. Marques et al. (2019) were able to detect the number of trees in the chestnut orchard with 99% accuracy using the combination of visible and NIR bands and canopy height model. Dong et al. (2020) used the local maxima method in their study to detect apple and pear trees and were able to determine the trees in the orchard with 99% accuracy. Again, Dong et al. (2020) obtained a producer accuracy value of 97.40% in apple trees and 98.0% producer accuracy in pears in the same study they carried out to determine the crown structures of trees in both apple and pear orchards. The user accuracies found in the study are 95.5% and 97.1%, respectively. Ok and Özdarıcı-ok (2018) found an F score value of over 92% in an integrated system study they carried out for the detection of citrus fruit trees from the digital surface model, extraction of crown borders and clustering.

Díaz-Varela et al. (2015) estimated the crown diameters of olive trees and obtained RMSE values of 0.32 m (R^2 = 0.58) and 0.28 m (R^2 = 0.22) for the two study areas, respectively. Castro et al., (2019) carried out a study to determine the earliest date for the appropriate measurement of architectural features of the olive tree using UAV images and object-based image analysis techniques. Within the scope of the study, the diameter and height of the olive tree were evaluated. The olive tree (*Olea europaea L.*), which belongs to the Oleaceae family, is a tree that has been cultivated since ancient times and never leaves its leaves during its development period (Zohary and Spiegel-Roy, 1975). More than 97% of the olive production areas in the world are located in the Mediterranean Basin. While Spain ranks first in the world in terms of olive production, Spain is followed by Greece, Italy and Turkey, respectively (Castro et al., 2019). While there were 80 600 000 trees bearing fruit and 1 100 000 tons of olive production (for table and oil) in 1990 in Turkey, the number of trees was 159 382 000 olive production (for table and oil) by 2020 (TÜİK, 2021).

Although satellite and ground based remote sensing techniques have been widely used in a number of plant

species, there is limited research on olive tree (Olea europaea L.) of dendrometric components. Since the development of reliable methods for calculating dentrometric parameters is an important key in evaluating the adaptation of trees to environmental conditions and/or the growing system. In this study it was aimed to determine dentrometric parameters (tree crown boundary crown area and tree height) of olive trees with the UAV.

2. Material and Method

2.1. Study area and data acquisition

The study area is located in Antalya Province, Konyaaltı, Akdeniz University Faculty of Agriculture, at 36° 53' 54'' N and 30° 38' 13'' E coordinates, 50 m above sea level and 3 km from the Mediterranean Sea. The experiment was carried out on 77 olive trees, which are twenty-five years old, belonging to the Memecik olive variety, located on a total area of 2766.76 m^2 (Figure 1).

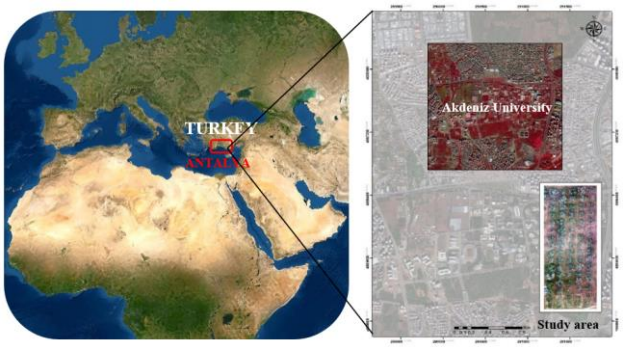

Figure 1. Study area overview

Unmanned aerial vehicle images obtained from the study area were taken in May 2017 at a flight height of 30 m and at a 2 m s^{-1} speed. The side and frontal overlap rate for all flight lines was 80%. Default values were used for all other parameters in the flight planning phase of the study. The UAV used in the study is DJI Phantom 3 Advanced which is 1280 g weight and has the flight time of about 23 minutes and a 12 MP camera (Figure 2).

Figure 2. The unmanned aerial vehicle used in the study

During the field studies of the research and the acquisition of terrestrial measurement data, the trees in the area were counted in the field. In addition, tree heights were measured with high precision using a total station (Topcon) and a prism. Trigonometric calculation method was used to obtain tree heights. In this method, the ground is assumed to be flat. (Ramli and Tahar, 2020). The work area is also located on a flat surface. The actual tree height was determined by this process in the field (Figure 3).

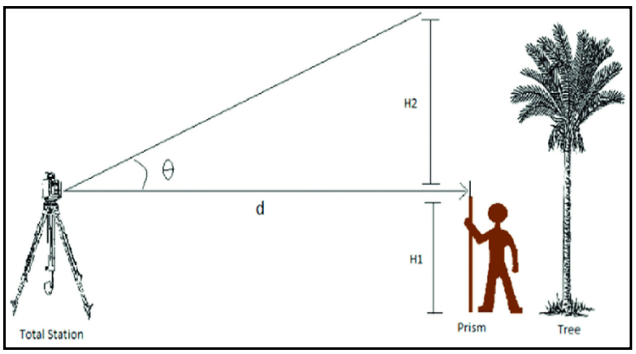

Figure 3. Plant Height Measurement Method in Land Conditions (Ramli and Tahar 2020)

2.2. Method

The study consists of basic processing steps of image processing, image analysis and evaluation (Figure 4). In the image analysis stage of the study, sub-process steps were carried out to determine the olive trees in the grove, to determine the tree crown borders, to calculate the tree crown areas and tree heights.

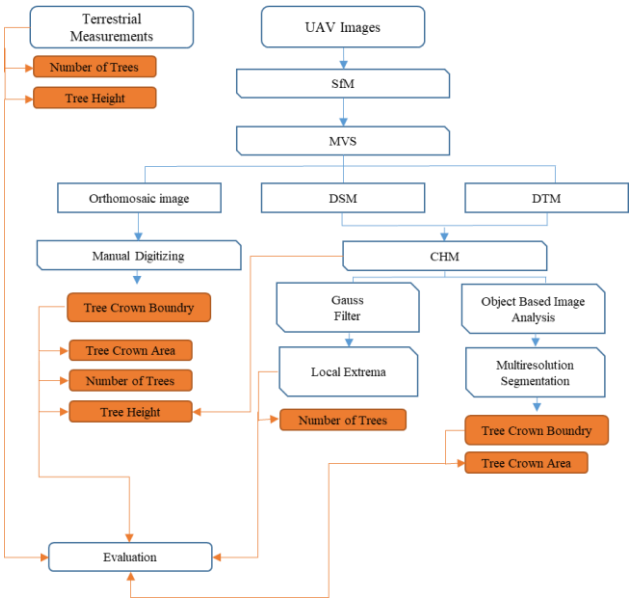

Figure 4. Flowchart

2.2.1. Image processing

The basic data used within the scope of the study are UAV images and terrestrial measurement values obtained from field inventory. For 83 UAV images obtained from the study area, firstly, orthomosaic image of the area, DSM

and DTM were created. For this process, Structure from Motion (SFM) and then Multi View Stereo (MVS) processes were performed in order to produce a 3D model from a series of images obtained with the UAV in Pix4Dmapper Pro (Pix4D Inc., Denver, USA) software. In the first sub-step of this stage, the Pix4Dmapper Pro software automatically performed the matching process and aligned the images by taking into account certain features (keypoints) present in all images to create connection points.

In the second sub-step of this stage, a dense point cloud and a three-dimensional textured mesh are produced. Finally, a DSM was created with the inverse distance weighting method based on the previously created point cloud. At this stage of the study, in addition to DSM, a DSM-based DTM was created using an orthorectified orthomosaic image and an additional module in Pix4Dmapper software. The parameter and processing settings applied to the UAV images during the image processing phase of the study are given in Table 1. While the resolution of the orthomosaic and DSM is 1.33 cm, the ground sampling distance (GSD) of the DTM is set to 5 times the GSD of the orthomosaic image, which is the optimum value in the Pix4Dmapper software.

Table 1. UAV data processing settings

Parameters	Settings
DSM and Orthomosaic Resolution	1xGSD (1.33[cm/pixel])
DSM Filters	Noise Filtering: yes Surface Smoothing: yes Type: Sharp
Raster DSM	Generated: yes Method: IDW Merge Tiles: yes
Orthomosaic	Generated: yes Merge Tiles: yes GeoTIFF Without Transparency: no Google Maps Tiles and KML: no
Raster DTM	Generated: yes Merge Tiles: yes
DTM Resolution	5xGSD (1.33[cm/pixel])
Time for DSM Generation	11m:22s
Time for Orthomosaic Generation	15m:31s
Time for DTM Generation	01m:59s

2.2.2. Image processing

With the high resolution orthomosaic image produced in the first stage of the study, tree crown borders were determined by manual digitization in a geographic information systems (GIS) and tree crown areas and tree numbers were determined by using these crown borders. ArcGIS software (Esri, California, USA) was used at this stage. The height of the trees in the study area was calculated by creating a CHM. In this context, a CHM of olive trees was produced using Equation 1.

$$CHM = DSM - DTM \quad (1)$$

At this stage, a Gaussian filter was applied to the CHM as the first operation. The Gaussian filter uses a kernel, which is a square matrix of values applied to image pixels (Trimble, 2014). With the Gaussian filter, each pixel value in the image is replaced by the average of the square area of the matrix centred on the pixel. With this filter, which is also called Gaussian blur, it is aimed to remove noise and details on the image. Then, the number of trees and their positions were determined by calculating the local maximums with the local extrema algorithm on this filtered image. The local extrema algorithm classifies the image objects that meet the local extrema condition to the smallest or largest feature value. This enables the determination of areas that fulfill the maximum or minimum condition within a defined area. In this study, maxima were chosen as the extrema type in the algorithm.

As another process in the study, object-based image analysis was used to determine the tree crown borders. In the object-based image analysis phase of the study, eCognition software (Trimble Inc., Sunnyvale, CA, USA) was used. The most important stage of object-based image analysis is the segmentation stage. Segmentation algorithms used for this purpose are used to divide certain objects in images into smaller image objects in order to separate them from other areas. The most used algorithm for this purpose is the multiresolution segmentation algorithm (MRS) (Drăguţ et al., 2014). The multiresolution segmentation algorithm is a bottom-up segmentation algorithm based on the binary region merging technique, as it successively combines pixels or existing image objects (Trimble, 2014). With this segmentation algorithm, average heterogeneity is minimized and homogeneity is maximized for a certain number of image objects. In the MRS algorithm, the scale parameter and the shape and compactness criteria must be entered. The scale parameter is used to optimize the size of the image objects, while the shape criterion is the relationship between the shape and colour criterion, and the compactness criterion is used to optimize the image objects in terms of integrity. In order to determine the tree crown borders and areas, the MRS algorithm, which is frequently used in object-based image analysis, was applied to the CHM image and the image was segmented (Trimble, 2014). Tree objects were determined by applying threshold values over these segments. The

height of the weeds in the study area was taken into account when determining the threshold value. The areas of these tree crowns, which were transferred to the GIS environment in vector data format, were also calculated.

2.2.3. Evaluation

In the last stage of the study, the relationships between UAV data and ground realities were correlated and the data were evaluated statistically. In this context, accuracy analysis was carried out between the number of trees determined by the local extrema algorithm and trees counted manually in the study area. Using the evaluated possible outcomes and the equations (from Eq.2 to Eq.5) below, the producer, user, and overall accuracy values and the F score were calculated (Ozdarici-Ok 2015; Yin and Wang, 2016; Dong et al., 2020).

$$PA = \frac{TP}{TP+FN} x\ 100 \quad (2)$$

$$UA = \frac{TP}{TP+FP} x\ 100 \quad (3)$$

$$F = \frac{2xPAxUA}{PA+UA} \quad (4)$$

$$OA = \frac{TP}{TP+FN+FP} x\ 100 \quad (5)$$

In addition, at this stage, evaluations were made according to the matching categories determined between the tree crown borders and crown areas, which were determined semi-automatically by the MRS algorithm, and the crown borders and areas that were manually extracted from the orthomosaic image. In order to determine the tree crown borders, six matching accuracy categories were used according to the spatial relationships between manually determined (reference) tree crowns and extracted tree crowns in the olive grove (Jing et al., 2012; Fang et al., 2016; Dong et al., 2020). These categories are matched, near matched, split, merged, wrong and missed (Figure 5).

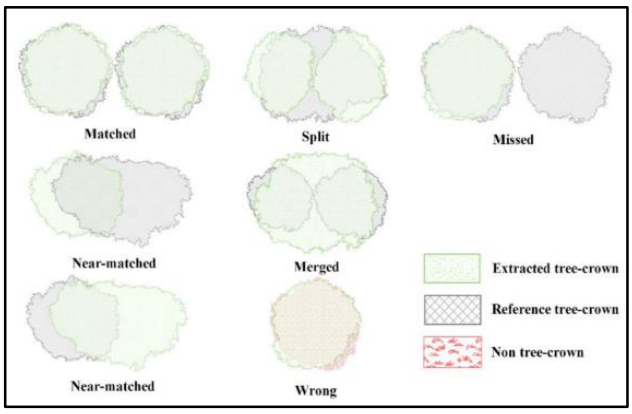

Figure 5. Tree crown matching categories (Dong et al., 2020)

Producer and user accuracy was calculated by using the formulas (from Eq.6 to Eq.9) given below for accuracy assessment in determining tree crown boundaries (Dong et al., 2020).

$$PA = \frac{E_{ma}}{E_e - E_{wr}} \times 100 \quad (6)$$

$$UA = \frac{R_{ma}}{R_e} \times 100 \quad (7)$$

$$E_e = E_{ma} + E_{nm} + E_{me} + E_{sp} + E_{mi} + E_{wr} \quad (8)$$

$$R_e = R_{ma} + R_{nm} + R_{me} + R_{sp} + R_{mi} \quad (9)$$

where E, extracted tree crown; R, reference tree crown; E_e, total number of tree crowns extracted; R_e, total number of reference tree crowns; ma, number of matching tree crowns; nm, number of near matched tree crowns; me, number of merge tree crowns; sp, number of split tree crowns; mi, number of tree crowns missed; wr number of wrong tree crowns.

In the correlation analysis, the r (Pearson correlation coefficient) value was calculated using Equation 10 as follows:

$$r = \frac{\sum_{i=1}^{n}(x_i - \bar{x})(y_i - \bar{y})}{(n-1)S_x S_y} \quad (10)$$

In Pearson's correlation coefficient equation, xi is the value of the x variable of the observation i; $\bar{x}$ is the sample mean of the x variable; Sx is the sample standard deviation of the variable x; yi is the y value of the observation i; $\bar{y}$ is the sample mean of the y variable; Sy shows the sample standard deviation of the variable y and n shows the number of observations. In order for the relationship between two variables to be considered statistically significant, the condition rist ≥ tα must be met (Çubukçu, 2015). In this context, the statistic (rist) of Pearson's correlation coefficient was calculated with Equation 11 as follows:

$$r_{ist} = r\sqrt{\frac{n-2}{1-r^2}} \quad (11)$$

where r_{ist} is the statistics of Pearson's correlation coefficient; r is Pearson's correlation coefficient and n is the number of observations. At this stage of the study, statistical analysis was carried out between the height data of each tree obtained by using the polygon and CHM, which were extracted from the high resolution orthomosaic image, and the height data obtained by terrestrial measurements from the TOPCON device.

3. Results and Discussion

After the image processing stage, which is the first stage of the study, the orthomosaic image of the area, DSM, DTM, CHM and tree crown borders obtained by manual digitization were produced. The obtained results are shown in Figure 6.

As can be seen in Figure 6, both vector format and raster format data sets were produced for the olive trees in the experimental area. Due to the high spatial resolution in the ortho mosaic image, all olive trees were precisely identified by visual analysis at this stage of the study. In addition, DSM and DTM data (Figure b and c) were produced from the UAV, and CHM data was produced by subtracting these data from each other (Figure d). Dentrometric properties of olive trees such as crown border, crown width and tree height were calculated precisely with the produced CHM.

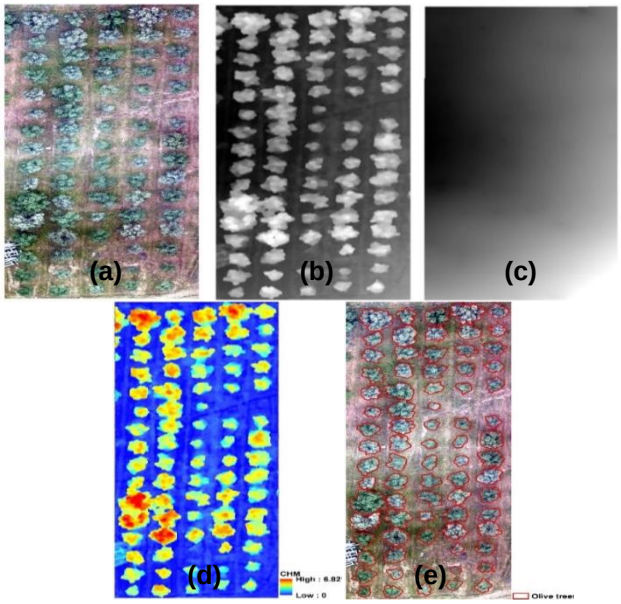

Figure 6. Orthomosaic image produced from UAV images (a); DSM (b); DTM (c); CHM (d); (e) Reference tree crown borders

3.1. Determination of tree numbers

Trees determined by the local maxima algorithm are shown in Figure 7 with red dots, and locally detected trees are shown with green dots. Three possible outcomes were evaluated within the scope of accuracy analysis performed between extracted trees and reference trees (Mohan et al., 2017; Dong et al., 2020). Based on these possible results, 75 trees were detected correctly (true positive-TP). According to the findings obtained at this stage, 3 trees were removed as false positive (FP).

Producer and user accuracy for the detection of olive trees was found to be over 96%, the F score was 98.04%, and the overall accuracy was 96.15% (Table 3).

Table 3. Accuracy evaluation results for tree numbers

Evaluation	Indicator
True Positive-TP	75
False Positive-FP	3
Producer Accuracy-PA (%)	100.00
User Accuracy-UA (%)	96.15
F Score (%)	98.04
Overall Accuracy (%)	96.15

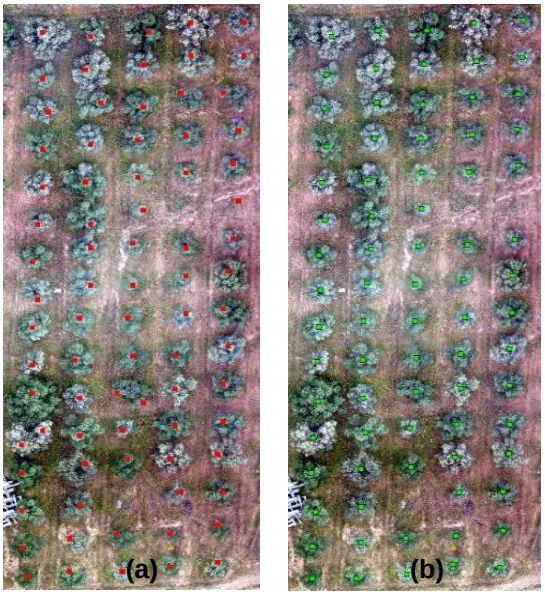

Figure 7. Extracted (a); and reference trees (b)

Findings from the study are similar to Dong et al 2020. It is thought that the reason for the mixing in three of the olive trees in the study area is due to the irregular crown structure of two of these trees. It was determined that the other FP tree was detected as a tree by the LM algorithm, although it was a different plant and was not an olive tree.

3.2. Determination of tree crown borders

In Figure 8, the results obtained according to the multiresolution segmentation algorithm are given. The tree segments formed according to the result of the object-based analysis and the tree crown borders extracted using these segments are seen. In addition, the reference tree crown borders produced by manual digitization over the very high resolution orthomosaic image are given in the figure below.

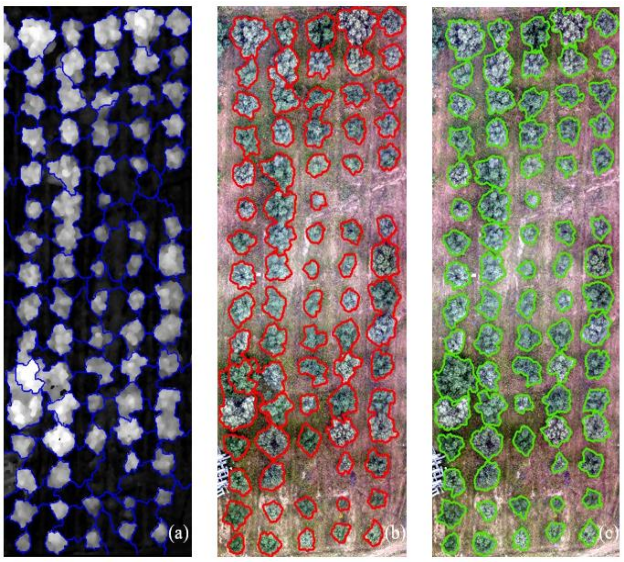

Figure 8. The result of the segmentation process (a); Extracted tree crowns (b); Reference tree crowns (c)

According to the six matching categories used to determine the tree crown borders, 63 trees crown borders were matched, while 6 trees crown borders were near matched. According to these findings, the producer accuracy is 85.14% and the user's accuracy is 81.82% (Table 4).

Table 4. Accuracy assessment results for tree crown borders

Evaluation	Indicator	Evaluation	Indicator
E_{ma}	63	R_{ma}	63
E_{nm}	6	R_{nm}	6
E_{me}	3	R_{me}	6
E_{sp}	0	R_{sp}	0
E_{mi}	2	R_{mi}	2
E_{wr}	0		

In the study, it was determined that there were some trees in the determination of the crown boundaries, as well as in the determination of the number of trees. It is thought that this is due to the irregularity in the crown structure of olive trees. During the MRS segmentation process, the result is that the structural condition of the trees reduces the quality of the process.

The data regarding the problems encountered in determining the number of trees and crown boundaries in the study are given in Figure 9. In Figure 9a, the determination of the number of trees and in Figure 9b the errors in determining the tree crown boundaries are given, and in Figure 9c, the irregularities in the structure of the trees that cause these errors are shown as an example.

3.3. Calculation of tree crown areas

The tree crown areas in the study area determined by manual digitization were calculated semi-automatically in the GIS environment. According to these tree crown areas, the maximum value in the area is 29.910 m^2, minimum value is 3.330 m^2 and the average value is 11.850 m^2 (Table 5).

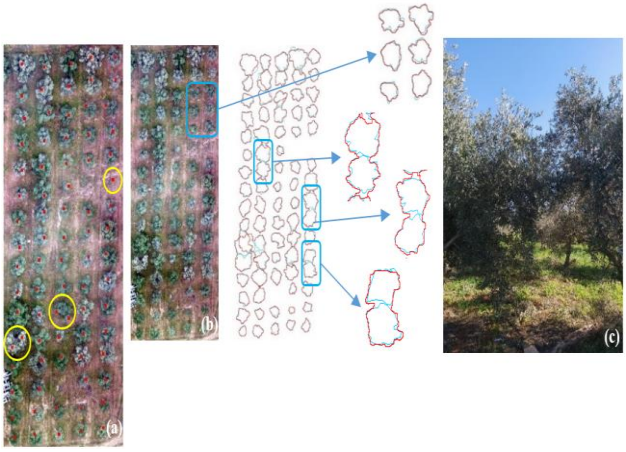

Figure 9. Errors encountered in tree detection

Correlation analysis was performed in terms of tree crown areas among 63 trees mapped according to 6 matching categories from manually determined tree crowns and extracted tree crowns. As a result of the calculations, Pearson's correlation coefficient (r) was 0.980 and Pearson's correlation coefficient statistics (r_{ist}) was 38.87. Since Pearson's correlation coefficient statistic was higher than the threshold value (t_α = 2.000), it was determined that Pearson's correlation coefficients were significant at the 95% confidence level (double-tailed) and there was a statistically positive relationship between the two variables.

According to the findings, it has been shown that the crown areas of olive trees can be calculated very accurately and reliably by using UAV. As in this study, Dong et al., 2020, Mohan et al., 2017 and Diaz-Varela et al., As the researchers stated in 2015, reliable results were obtained.

3.4. Calculation of tree heights

Reference tree heights were obtained by ground measurements using the TOPCON device. According to the findings, the maximum tree height was determined as 6,180 m, the minimum tree height was 1,880 m, and the mean tree height was 3,929 m for the reference values. The calculated CHM values were determined as the maximum tree height of 6.820 m, the minimum tree height of 2.550 m and the mean tree height of 4.362 m. (Table 6).

Table 5. Supplementary statistics values for tree crown areas

Max* (m^2)	Min* (m^2)	Mean* (m^2)	Median* (m^2)	SD* (m^2)	CV* (%)
29.910	3.330	11.850	11.430	5.181	43.583

**Max, maximum tree crown area; Min, minimum tree crown area; Mean, mean tree crown area; Median, median tree crown area; SD, standard deviation; CV, coefficient variation.*

Pearson's correlation coefficient (r) and Pearson's correlation coefficient statistic (r_{ist}) between these extracted tree heights and the height data obtained by terrestrial measurements were calculated using Equation 2 and Equation 3. In terms of tree heights, Pearson's correlation coefficient (r) was calculated as 0.918 and Pearson's correlation coefficient statistic (r_{ist}) was calculated as 20.10. In this case, it is seen that Pearson's correlation coefficient statistic is higher than the $t\alpha$ threshold (20.10 > 1.990). According to this result, it was determined that there was a statistically significant positive relationship between the two variables in terms of double-tailed tree heights at the 95% confidence level.

In the study, statistically significant results were obtained between the precise local measurement studies in determining the height of the olive tree and the heights

Table 6. Calculation of tree heights

Supplementary statistics values for tree heights (Reference)						Supplementary statistics values for tree heights (Calculated with CHM)					
Max* (m)	**Min* (m)**	**Mean* (m)**	**Median* (m)**	**SD* (m)**	**CV* (%)**	**Max* (m)**	**Min* (m)**	**Mean* (m)**	**Median* (m)**	**SD* (m)**	**CV* (%)**
6.180	1.880	3.929	3.850	0.770	19.605	6.820	2.550	4.362	4.290	0.801	18.356

*Max, maximum tree height; Min, minimum tree height; Mean, mean tree height; Median, median tree height; SD, standard deviation; CV, coefficient variation.

calculated semi-automatically from CHM. According to these findings, it has been revealed that UAVs can give reliable results in estimating the height of the trees.

4. Conclusion

As a result of the research, 96.15% accuracy was obtained in the detection of individual olive trees distributed in the olive plot, while an object or pixel group was incorrectly detected as a tree, and two trees could not be determined at all (Figure 9a). A high value was obtained in the determination of olive trees, close to the values found by Castro et al. (2019), Marques et al. (2019) and Dong et al. (2020).

In determining the single tree crown borders, 81.82% user accuracy and 85.14% producer accuracy were determined. In addition, statistically high correlations were found in the determination of tree crown areas (r = 0.980) and heights (r = 0.918) of individual trees. On the other hand, in determining the tree crown borders, it was determined that some trees matched quite well, but the six trees in the reference data were merged into a single tree (Figure 9b). The reason for this was considered to be due to the fact that the tree crowns in the area were intertwined as in the image (Figure 9c).

According to the findings obtained from the study, it has been revealed that applications such as individual tree detection, determination of the crown borders of the trees, reliable calculation of crown areas and heights, which will be made in the perennial agricultural production environment with UAV, give extremely successful results. The values obtained in the determination of tree parameters (crown areas and heights) are close to the values obtained by Mu et al. (2018) and Dong et al. (2020) and were found to be higher than the values obtained by Díaz-Varela et al. (2015) and Castro et al. (2019).

As a result of this study, in future studies to be carried out with unmanned aerial vehicles in perennial production environments, it is recommended to include LIDAR data that can be mounted on UAVs in the analysis in order to take into account the different developmental stages of the plant and also to demonstrate the working sensitivity more clearly. It is thought that the precise determination of plant biomass, which is especially related to plant yield, will provide important advantages in yield estimation studies.

Author Contributions

Mesut Çoşlu: Conceptualization, Methodology, Software, Validation, Formal Analysis, Investigation, Material Supply, Original Draft Writing, Review and Editing, Visualization.
Namık Kemal Sönmez: Methodology, Validation, Original Draft Writing, Review and Editing, Supervision, Observation, Advice.

Conflict of Interest

As the authors of this study, we declare that we do not have any conflict of interest statement.

Ethics Committee Approval

As the authors of this study, we declare that we do not have any ethics committee approval.

Kaynaklar

Carolan, M. (2017). Publicising food: big data, precision agriculture, and co-experimental techniques of addition: publicising food. *Sociollogia Ruralis*, *57*, 135-154. https://doi.org/10.1111/soru.12120

Castro, A. I., Rallo, P., Suárez, M. P., Torres-Sánchez, J., Casanova, L., Jiménez-Brenes, F. M., Morales-Sillero, A., Jiménez, M. R., & López-Granados, F. (2019). High-throughput system for the early quantification of major architectural traits in olive breeding trials using UAV images and OBIA techniques. *Frontiers in Plant Science*, *10*, 1472. https://doi.org/10.3389/fpls.2019.01472

Çubukçu, K. M. (2015). *Planlamada ve coğrafyada temel istatistik ve mekânsal istatistik kitabı*. Nobel Akademik Yayıncılık, Yayın No:1097, Ankara.

Das, U. (2018). Precision farming a promising technology in horticulture: a review. *International Journal of Pure Applied Bioscience*, *6*, 1596-1606. https://doi.org/10.18782/2320-7051.3088

Demir, N., Sönmez, N. K., Akar, T., & Ünal, S. (2018). Automated measurement of plant height of wheat genotypes using a DSM derived from UAV imagery. *MDPI Proceedings*, *2*, 350-350. https://doi.org/10.3390/ecrs-2-05163

Díaz-Varela, R. A., de la Rosa, R., León, L., & Zarco-Tejada, P. J. (2015). High-resolution airborne UAV imagery to assess olive tree crown parameters using 3D photo reconstruction: Application in breeding trials. *Remote Sensing*, *7*, 4213-4232. https://doi.org/10.3390/rs70404213

DJI (2021). Phantom 3 advanced specs. Access address https://www.dji.com/phantom-3-adv/info

Dong, X., Zhang, Z., Yu, R., Tian, Q., & Zhu, X. (2020). Extraction of information about individual trees from high-spatial-resolution UAV-acquired images of an orchard. *Remote Sensing*, *12*, 133. https://doi.org/10.3390/rs12010133

Drăguţ, L., Csillik, O., Eisank, C., & Tiede, D. (2014). Automated parameterisation for multi-scale image segmentation on multiple layers. *ISPRS Journal of Photogrammetry and Remote Sensing*, *88*, 119-127. https://doi.org/10.1016/j.isprsjprs.2013.11.018

Fang, F., Im, J., Lee, J., & Kim, K. (2016). An improved tree crown delineation method based on live crown ratios from airborne LIDAR data, *GIScience & Remote Sensing*, *53*, 402-419. https://doi.org/10.1080/15481603.2016.1158774

Jing, L., Hu, B., Li, J., & Noland, T. (2012). Automated delineation of individual tree crowns from LIDAR data by multi-scale analysis and segmentation. *Photogrammetric Engineering and Remote Sensing*, 78(12), 1275-1284. https://doi.org/10.14358/PERS.78.11.1275

Marques, P., Pádua, L., Adão, T., Hruška, J., Peres, E., Sousa, A., & Sousa, J. J. (2019). UAV-based automatic detection and monitoring of chestnut trees. *Remote Sensing*, *11*, 855. https://doi.org/10.3390/rs11070855

Matese, A., Capraro, F., Primicerio, J., Gualato, G., Di Gennaro, S. F., & Agati, G. (2013). Mapping of vine vigor by UAV and anthocyanin content by a non-destructive fluorescence technique. In Proceedings of the 9th European Conference on Precision Agriculture (ECPA), Lleida, Spain, 7–11 July.

Mu, Y., Fujii, Y., Takata, D., Zheng, B., Noshita, K., Honda, K., Ninomiya, S., & Guo, W. (2018). Characterization of peach tree crown by using high-resolution images from an unmanned aerial vehicle. *Horticulture Research*, *5*, 74. https://doi.org/10.1038/s41438-018-0097-z

Mohan, M., Silva, C. A., Klauberg, C., Jat, P., Catts, G., Cardil, A., Hudak, A. T., & Dia, M. (2017). Individual tree detection from unmanned aerial vehicle (UAV) derived canopy height model in an open canopy mixed conifer forest. *Forests*, *8*, 340. https://doi.org/10.3390/f8090340

Ozdarici-Ok A. (2015). Automatic detection and delineation of citrus trees from VHR satellite imagery. *International Journal of Remote Sensing*, *36*, 4275–4296. https://doi.org/10.1080/01431161.2015.1079663

Ok, A. O. & Ozdarici-Ok, A. (2017). Detection of citrus trees from UAV DSMs. *In Proceedings of the ISPRS Annals of the Photogrammetry, Remote Sensing and Spatial Information Sciences*, Hannover, Germany, *4*, 27-34. https://doi.org/10.5194/isprs-annals-IV-1-W1-27-2017

Ok, A. O. & Ozdarici-Ok, A. (2018). 2-D delineation of individual citrus trees from UAV-based dense photogrammetric surface models. *International Journal of Digital Earth*, *11*, 583-608. https://doi.org/10.1080/17538947.2017.1337820

Ok, A. O., & Ozdarici-Ok, A. (2018). Dijital yüzey modelinden turunçgil meyve ağaçlarinin tespiti, çıkarımı ve kümelenmesi: bütünleşik bir sistem, VII. UZAL-CBS Sempozyumu (Birinci En İyi Sözlü Sunum Ödülü). VII. UZAL-CBS Sempozyumu, Eskişehir, Türkiye.

Ramli, M. F., & Tahar, K. N. (2020). Homogeneous tree height derivation from tree crown delineation using seeded region growing (SRG) segmentation. *Geo-Spatial Information Science*, *23*(3), 195-208. https://doi.org/10.1080/10095020.2020.1805366

Sönmez, N. K., Çoşlu, M., & Demir, N. (2021). Farklı insansız hava araçlarından (İHA) elde edilen veriler ile buğday bitkisinin boyunun belirlenmesi. *Mediterranean Agricultural Sciences*, *34*(2), 195-203. https://doi.org/10.29136/mediterranean.823440

Sunar, F., Özkan, C., & Osmanoğlu, B. (2013). *Uzaktan algılama* (2. Baskı). T.C. Anadolu Üniversitesi, Yayın No: 2320, Açıköğretim Fakültesi Yayın No:1317, Eskişehir.

Trimble, (2014). *eCognition developer 9.0 reference book.* Trimble Germany GmbH, Arnulfstrasse 126, D-80636 Munich, Germany.

TÜİK (2021). Zeytin üretimi, 1988-2020. Access address https://data.tuik.gov.tr/Search/Search?text=zeytin

Yin, D., & Wang, L. (2016). How to assess the accuracy of the individual tree-based forest inventory derived from remotely sensed data: A review. *International Journal of Remote Sensing*, *37*, 4521-4553. https://doi.org/10.1080/01431161.2016.1214302

Zohary, D., & Spiegel-Roy, P. (1975). Beginnings of fruit growing in the old world. *Science, 187*, 319-327. https://doi.org/10.1126/science.187.4174.319.